

EXPERIMENTAL EVIDENCE OF DIFFERENT INTERMEDIATE WETTING STATES

A. Skauge, K. Spildo, L. Høiland, B. Vik, and B. Ottesen
Centre for Integrated Petroleum Research, U of Bergen, Norway

This paper was prepared for presentation at the International Symposium of the Society of Core Analysts held in Abu Dhabi, UAE, 5-9 October, 2004

ABSTRACT

Earlier studies have concluded that different intermediate-wetting states can be identified from analysis of USBM and Amott-Harvey wettability indices. The analysis can distinguish between fractional wet (FW) and classes of mixed-wet state, mixed-wet large (MWL) and mixed-wet small (MWS). The wettability analysis have earlier identified 13 reservoirs where five could be grouped as MWL, four as FW, and four as MWS. The different groups have shown several important differences with respect to as examples core cleaning, residual oil saturation and endpoint relative permeability relations.

Still, there is a need to experimentally verify that the local wetting sites confirm the intermediate-wetting structure identified by USBM and Amott-Harvey wettability indices. This paper addresses evidence of different intermediate-wetting states from analysis of reservoir core material.

Cores from oil reservoirs showing mixed-wet large (MWL) and mixed-wet small (MWS) behaviour have been studied by ESEM. SEM analysis and thin sections showed that a reservoir identified as having MWL type wettability had large pores with surfaces mostly consisting of quartz. Smaller pores and pore throats contained clays. The ESEM analysis identified quartz as intermediate-wet, while the clay in this case was water-wet. Another reservoir was identified as mixed-wet small, and in this case only the high surface area material feldspar and clay deviated from water-wet behaviour. Combined with field studies in the literature these results confirm the classification resulting from comparing USBM to Amott-Harvey wettability indices.

INTRODUCTION

Wettability is known to influence fluid flow processes in porous media. Most reservoirs are neither strongly water-wet nor strongly oil-wet, but rather fall into the large group of intermediate-wet state. Special core analysis of intermediate-wet rock shows a wide variation in properties like end-point saturation, capillary pressure and relative permeability. We have earlier pursued an approach to improve the understanding of the intermediate-wet state by dividing the intermediate-wet group into three sub-classes [1-3]; fractional-wet (FW), where oil- and water-wet sites are random with respect to pore size, and two mixed-wet classes defined by water- and oil-wet pores that are sorted by pore size. MWL (mixed-wet large) is defined by oil-wet large pores, while MWS (mixed-wet small) refers to smaller pores being oil-wet.

No direct measurements of the wettability of reservoir cores are available, instead the Amott [4], USBM [5] and combined Amott/USBM methods are commonly employed empirical estimates for wettability. While both the Amott and USMB methods [6] are based on displacement studies, the former is largely governed by spontaneous displacement processes while the latter is dependent on the energy involved in forced displacement processes. Therefore, although they have been used interchangeably in the literature, it is not obvious what the relationship between these two measures of core wettability should be.

Dixit *et al.* [7-8] have suggested analytical relationships between I_{AH} and I_{USBM} for various wetting scenarios. In their approach they distinguished between wettability types based on the fraction of oil-wet pores and their distribution within the pore space in the following ways (see Fig. 1):

- *Fractionally-wet (FW)* where the oil-wet pores are uncorrelated to size
- *Mixed-wet large (MWL)* where the largest pores are oil-wet
- *Mixed-wet small (MWS)* where the smallest pores are oil-wet

When calculating the relationships, a uniform pore-size was assumed, accessibility issues were neglected and phase-trapping was not accounted for. This simplified approach predicts $I_{AH} = I_{USBM}$ for the FW case over the range $-0.5 < I_{AH} < 0.5$, independent of the type and range of pore size distribution (PSD) or relationship between pore size and – volume. For either type of mixed-wet systems, however, both the type and range of PSD and the volume exponent will affect the relationship between the two wettability indices. The calculated $I_{AH} - I_{USBM}$ relationship is predicted to lie above the $I_{AH} = I_{USBM}$ line for MWL systems, and below for MWS systems. This relationship was also confirmed by simulations on more realistic 3D pore networks taking into account both accessibility and phase-trapping issues [7-9]. Arguments for the possible existence of FW, MWS and MWL porous media, based on a discussion of pore level displacement mechanisms and wettability alteration, will be discussed later.

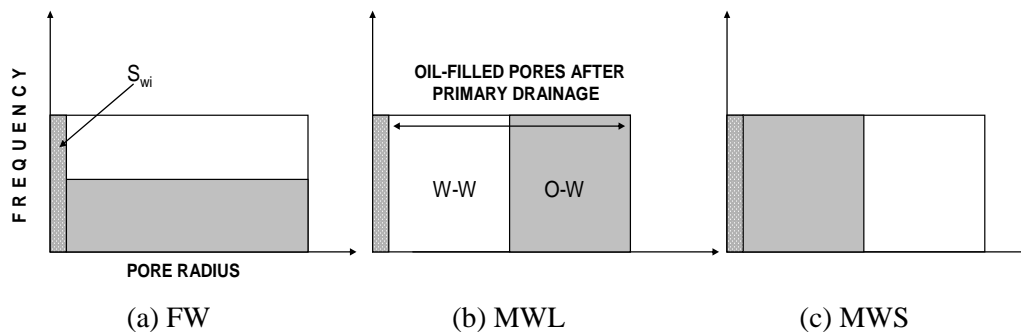


Figure 1: The filled area is the fraction, f , of oil-wet pores which is either located (a) independent of size in the fractional-wet (FW) state, (b) in the largest oil-filled pores in the mixed-wet large (MWL) wettability-type, or (c) in the smallest oil-filled pores for the mixed-wet small (MWS) class. Note that the smallest pores are not invaded by oil during primary drainage and thus remain water-wet.

EXPERIMENTAL

In thin section imaging, a resin was used to fill the void pore space and to eliminate clay smearing when cutting and polishing the samples. Both SEM and ESEM were used to analyse mineralogy and local wetting properties. The ESEM used condensation of water to visualise if water appeared as drops on the surface (less water-wet), or as a water film condensed on the surface (water-wet). The water film was seen as whitening of the edges of the solid surface due to refraction of the water films.

RESULTS AND DISCUSSIONS

Theoretical considerations - Why should FW, MWL, and MWS exist ?

The pressure difference across the oil-water interface, i.e. the capillary pressure, is given by the Young-Laplace equation:

$$P_c = P_o - P_w = \sigma \left(\frac{1}{R_1} + \frac{1}{R_2} \right) = \sigma C \quad (1)$$

In Eq. (1) σ is the interfacial tension, R_1 and R_2 are the principal radii of curvature, and C is the curvature of the fluid interface. For an oil-water interface in a cylindrical pore the principal radii of curvature are equal to the radius of the inscribed circle, R . For a strongly water-wet pore P_c is therefore given by $P_c = 2\sigma/R$.

When oil displaces water from an originally water filled, strongly water-wet reservoir, the pores with the lowest capillary entry pressure (i.e. the largest pores) are entered first. Water is then displaced from successively smaller pores until a maximum capillary pressure is reached. Following this primary drainage process water remains as films coating the pore walls and in the smallest pores. It is widely accepted that the extent of wettability alteration that occur in oil-filled pores after primary drainage largely depend on the stability of these pore-coating, thin films. If they become unstable and break, wettability can change by adsorption of crude oil components directly on the rock surface [10-14].

The disjoining pressure, $\Pi(h)$, is the force acting between two interfaces separated by a thin film of thickness h . When the disjoining pressure is positive the two interfaces repel each other and the film is stable, whereas when it is negative the interfaces attract each other and the film is unstable. There are three major factors contributing to the disjoining pressure; electrostatic interactions, van der Waals interactions and hydration forces [10,15]. The origin of these forces and how they vary with fluid composition and mineralogy is described in more detail elsewhere (see for example [10,15]). The disjoining pressure isotherm (see Fig. 2) describes how this parameter varies with film thickness at constant temperature. The disjoining pressure increases as the film thickness decreases until the local maximum value, Π_{\max} , is reached. This corresponds to a critical capillary pressure, P_c^* , for film rupture; when P_c exceeds P_c^* the film becomes unstable and break. In a real porous medium where both fluid composition and mineralogy may

vary with time and/or position, the disjoining pressure isotherm is likely to vary accordingly. In the following, however, we will assume for simplicity that the same disjoining pressure isotherm applies irrespective of pore size and shape for a porous media with a given average fluid composition and mineralogy. This means that the same Π_{\max} applies everywhere.

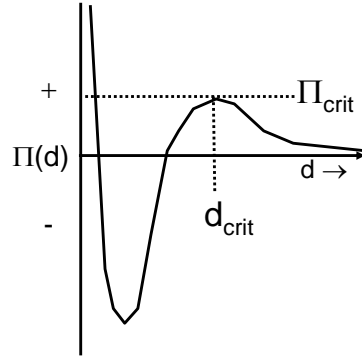


Figure 2: Disjoining pressure isotherm showing how the positive disjoining pressure increases as the interfaces approach each other (i.e. repulsive force increases) until a critical disjoining pressure (Π_{crit}) is reached at a given critical separation distance (d_{crit}). If the film thins further the disjoining pressure changes from positive to negative (attraction), and the film collapses.

Consider now the case of films in pores with different shapes. Figure 3 displays three different pore shapes; star-shaped, circular and triangular. These pores will give rise to convex, concave and planar films, respectively. By definition the curvature is negative for convex films, positive for concave films and zero for planar films. Suppose that you have a large/small pair of circular pores with the oil-water interface in the smallest pore as shown in Figure 4. Let the radius of the large pore be R_L and that of the small pore be R_S . The bulk oil (P_o) and water pressure (P_w) is the same throughout the system and thus $(P_c)_{\text{bulk}}$ is given by the curvature of the bulk interface in the small pore that has just been entered. In the films, however, the water pressure is larger than the bulk water pressure by an amount equal to the disjoining pressure; Π_L and Π_S for the large and small pore, respectively. The capillary pressure across the film in the large pore can be expressed as

$$(P_c)_{\text{film,L}} = P_o - (P_w + \Pi_L) = \frac{\sigma}{R_L} \quad \text{i.e.} \quad \Pi_L = (P_c)_{\text{bulk}} - \frac{\sigma}{R_L} \quad (2)$$

and in the small pore as

$$(P_c)_{\text{film,S}} = P_o - (P_w + \Pi_S) = \frac{\sigma}{R_S} \quad \text{i.e.} \quad \Pi_S = (P_c)_{\text{bulk}} - \frac{\sigma}{R_S} \quad (3)$$

This gives the following equations for the disjoining pressures

$$\Pi_L = \sigma \left(\frac{2}{R_S} - \frac{1}{R_L} \right) \quad (4)$$

$$\Pi_S = \frac{\sigma}{R_S} \quad (5)$$

Since $R_L > R_S$, it follows that $\Pi_L > \Pi_S$, and the disjoining pressure in the large pore is higher than in the small pore. Since the disjoining pressure is highest in the large pore, this will reach the critical value Π_{\max} first. Consequently, wettability is more easily changed in the large pores, giving rise to the *mixed-wet large (MWL)* wettability class.

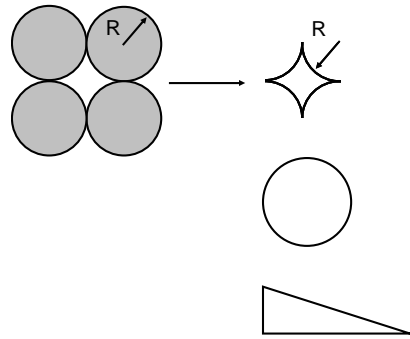


Figure 3: Different pore shapes give rise to different pore surface curvatures (from top to bottom); convex (star-shaped pore), concave (circular pore) and flat (triangular pore).

Similar arguments apply if you have a large/small pair of star-shaped or triangular pores, however, the capillary pressure across the film differs. For the star-shaped pores the curvature of the water films is negative by definition so that

$$\Pi_1 - \frac{\sigma}{R_1} = \Pi_2 - \frac{\sigma}{R_2} \quad \text{i.e.} \quad \Pi_1 = \Pi_2 + \sigma \left(\frac{1}{R_1} - \frac{1}{R_2} \right) \quad (6)$$

Since $R_L > R_S$, it follows that $\Pi_L < \Pi_S$, and the disjoining pressure in the small pore is higher than in the large pore. In this case the small pore will reach Π_{\max} first, wettability is more easily changed in the large pores, and we have a *mixed-wet small (MWS)* system. If the pore walls are flat, such as in a triangular pore, the water films have zero curvature. In this case $\Pi_L = \Pi_S$ and both small and large pores will reach Π_{\max} at the same time. Wettability is therefore uncorrelated to size in accordance with the *fractional-wet (FW)* scenario.

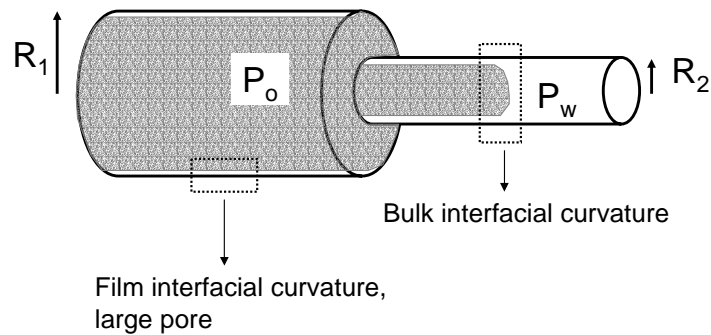


Figure 4: Large pore with radius R_1 followed by small pore with radius R_2 . Note that the shape of the film and bulk interfaces is fundamentally different. At the oil-water film interface, one of the radii of curvature approaches infinity ($C_1 = 1/R_1$ and $C_2 = 1/R_2$), whereas at the bulk oil water interface the two are equal ($C = 2/R_2$).

Having established the potential existence of FW, MWS and MWL porous media, the question remains as to whether or not these wettability states exist in oil reservoirs? In a data base of North Sea oil fields, it was found that thirteen reservoirs had enough I_{USBM} and I_{AH} data to determine the state of intermediate wettability [1]. In the present paper this data base has been extended to include more data for each field. Furthermore, we discuss whether this classification can explain the wide variation seen in special core analysis (SCAL) properties such as remaining oil saturation, endpoint relative permeability etc. on intermediate-wet reservoirs.

Reservoir core wettability

The wettability analysis combining I_{USBM} and I_{AH} has earlier [1] identified 13 reservoirs where five could be grouped as MWL, four as FW, and four as MWS. Some important results [3] include different effects of core cleaning, and it was also found that the average waterflood remaining oil saturation, S_{orw} , was lowest for the MWL cores compared to the other intermediate wetting states. A revisit of the literature shows a couple of cases where either local wetting has been identified or there are data for both I_{USBM} and I_{AH} .

Evidence of mixed-wet large (MWL)

Conventional mixed-wet is often described as MWL. The argument is as follows; the reservoir is assumed initially water-wet. Oil then migrates into the reservoir in a primary drainage process, and the oil-wet fraction is expected to be in the larger pores that are invaded by primary drainage. However, as discussed earlier, if the effect of pore geometry is taken into consideration one can argue that the oil-wet sites can be in the smaller oil invaded pores.

A thin section image of core material from a MWL reservoir is shown in Fig. 5. The pore space appears to be built up of large grains of quartz, mica and K-feldspar with flat

surfaces, as well as pore filling kaolinite. The pore filling clays contain small pores, but it is difficult to attribute a specific geometry to the micropores.

In order to detect the wetting properties of the mineral constituents, ESEM measurements were performed. Kaolinite and mica (Figures 9-10), show strongly water-wet behaviour from the ESEM. The condensation of water was seen as a whitening of grain edges due to water films, but only very few, small water droplets were seen. In contrast, the quartz and feldspar show mainly condensed water droplets on the surface (Figures 7-8). The more water-wet kaolinite located in the smaller pores is consistent with the MWL behaviour reported in earlier studies [1-3].

Salathiel [16] described what he called a mixed-wettability condition where “the fine pores and grain contacts would be preferentially water-wet and the surfaces of the larger pores would be strongly oil-wet”. He argued that if the oil-wet surfaces were continuous throughout the rock, this would explain the low residual oil saturations observed in an East Texas field. The measured wettability index was in the vicinity of zero. This type of mixed-wettability would be regarded as MWL.

Hamon [17] discusses the field-wide variation of wettability. The wettability is found to vary with height above free water level and permeability. The reservoir was analysed as more oil-wet at higher permeability and also at higher structural position (lower S_w) in the reservoir. Hamon found a weak trend between wettability and clay content; larger clay amounts were associated with more water-wet samples and smaller pores. No clear relationship between mineralogy and wettability was found, and thus he proposed that the effect of clays on pore geometry is larger than their effect on pore mineralogy. The residual oil saturation was higher closer to the water contact, and maximum oil recovery was found at $I_w=0$ and for higher permeability.

Evidence of fractional-wet (FW)

Fractional wettability would be reflected as spot like oil-wet sites on the surface. The origin of this wetting state could be because of precipitation, variation in mineralogy, or, as discussed, when the pore shape consists of flat surfaces.

One case from the literature which shows strong evidence of wettability state is Prudhoe Bay, Jerauld and Rathmell [18]. Dalmatian wettability was detected from analyses of Prudhoe Bay rock material where both oil- and water-wet regions are seen from ESEM even in the same pore. That is, the local wetting sites have an extension that is less than the size of the pore. Data from cryo-SEM shows that oil sticks to kaolinite higher on the structure and intermittently to quartz and chert. The wettability of kaolinite (oil-wet) is opposite to the reservoir discussed by Hamon [16]. Maximum oil recovery for Prudhoe Bay rock is found for $I_w = 0$ and the capillary forces were very weak. There was a trend towards more oil-wet with distance from the FWL, and also increasing oil-wet at higher S_w .

Evidence of mixed-wet small (MWS)

Mixed-wet small is regarded as a more unconventional mixed-wet state. But as argued earlier the water film will break first in the smaller pores when the curvature of the pore surface is convex (“star shaped” pores). Figure 6 is a thin section image of core material from a reservoir classified as MWS from comparing I_{USBM} and I_{AH} . Compared to the thin section picture of MWL core material, the curvature of the pore surfaces in the MWS sample is mostly convex. This is consistent with the theoretical analysis discussed earlier where smaller, “star shaped” pores are likely to become oil-wet. Contrary to the MWL case, it was not possible to attribute a specific mineral to the smaller pores. ESEM analysis (Figure 11-14) revealed that quartz in this case was more water-wet than for the MWL case. However, some of the higher surface area minerals such as mica was less water-wet, and may explain the mixed-wet small behaviour detected from wettability indices.

Rueslåtten *et al.* [19] found remaining oil saturation in small pores associated with kaolinite. In their study they characterised three North Sea cores and their twin plugs using I_{AH} , I_{USBM} wettability tests as well as cryo-SEM and NMR. Based on the values of I_{AH} and I_{USBM} , two of these plug sets would be classified as MWS while one would be classified as MWL. Incidentally, it was in the two MWS cores that remaining oil saturation was found in the small pores. In the MWL cores, oil was hardly detected in the fine pores. This is clear experimental indications that the MWL and MWS core states exist in reservoirs.

CONCLUSIONS

The theoretical considerations around different pore shapes argue that the three intermediate wetting states, FW, MWL, and MWS is possible for a porous medium.

Combining data from the literature with this study and earlier work show experimental evidence for the existence of the three wetting states.

Pore imaging by thin section analysis, ESEM and Cryo-SEM can be a useful tool in analysis of local wetting state. However, other additional experimental data like the wettability indices; I_{USBM} and I_{AH} is needed to differentiate between the classes of intermediate wetting state.

ACKNOWLEDGEMENTS

We would like thank Johannes Rykkje at Hydro for help with the ESEM analysis, and Prof. Kenneth Sorbie at Heriot Watt University for helpful discussions of pore scale wetting transitions.

REFERENCES

1. Skauge, A., and Ottesen, B., "A Summary of Experimentally derived Relative Permeability and Residual Saturation on North Sea Reservoir Cores," paper SCA 2002-12, paper presented at the International Symposium of the SCA, Monterey, CA, Sept. 2002.
2. Skauge, A., Vik, B., Spildo, K., and Ottesen, B., "Analysis of Intermediate Wettability", paper presented at the IEA 24th Annual Workshop & Symposium in Regina, Canada, Sept. 2003.
3. Skauge, A., Ottesen, B, Vik, B, "Variation of Special Core Analysis Properties for Intermediate Wet Sandstone Material," SCA 2003-5, paper presented at the International Symposium of the SCA, Pau, France, Sept. 2003.
4. Amott, E., "Observations Relating to the Wettability of Porous Rock," Petroleum Transactions, (1958) 156.
5. Donaldson, E.C., Thomas, R.D., Lorenz, B.P., "Wettability Determination and Its Effect on Oil Recovery," SPE Journal, (1969) 13.
6. Sharma, M.M., Wunderlich, R.W., "The Alteration of Rock Properties due to Interactions with Drilling Fluid Components," paper SPE 10111, presented at the SPE Annual Conference and Exhibition, Las Vegas, NV, Sept. 1985.
7. Dixit, A.B., Buckley, J.S., McDougall, S.R., and Sorbie, K.S., "Core wettability: "Should I_{AH} be equal to I_{USBM} ?," paper SCA 9809 presented at the International Symposium of the SCA, the Hague, the Netherlands, Sept. 1998.
8. Dixit, A.B., Buckley, J. S., McDougall, S. R., Sorbie, K.S., "Empirical Measures of Wettability in Porous Media and the Relationship Between them Derived from Pore-Scale Modelling," Transport in Porous Media, **40** (2000) 27.
9. Man, H. N., Jing, X. D., "Network Modelling of Mixed-Wettability Electrical Resistivity, Capillary Pressure and Wettability Indices," J. Petroleum Science Eng., **33** (2002) 101.
10. Hirasaki, G.J., "Wettability: Fundamentals and Surface forces," paper SPE/DOE 17367, presented at the SPE/DOE Symposium on IOR, Tulsa, OK, April 1988.
11. Buckley, J.S., K. Takamura, and N.R. Morrow, "Influence of Electrical Surface Charges on the Wetting Properties of Crude Oils," SPE Res. Eng., Aug. (1989) 332.
12. Kovscek, A.R., H. Wong, and C.J. Radke, "A Pore-level Scenario for the Development of Mixed Wettability in Oil Reservoirs," AIChE Journal, **39** (1993) 1072.
13. Dubey, S.T. and P.H. Doe, "Base number and wetting properties of crude oils," SPE Res. Eng., Aug. (1993) 195.
14. Basu, S. and M.M. Sharma, "Characterization of Mixed-Wettability States in oil Reservoirs by AFM," SPE Journal, **2** (1997) 427.
15. Melrose, J.C., "Interpretation of Mixed Wettability States in Reservoir Rocks," Paper SPE 10971, presented at the SPE Annual Conference and Exhibition, New Orleans, LA, Sept. 1982
16. Salathiel, R.A., "Oil Recovery by Surface Film drainage in Mixed-Wettability Rocks," J. Petroleum Tech., Oct. (1973) 1216.
17. Hamon, G.: "Field-wide variation of wettability", paper SPE 63144, presented at the SPE Annual Conference and Exhibition, Dallas, TX, Sept. 2000.

18. Jerauld, G.J., and Rathmell, J.J.: "Wettability and relative permeability of Prudhoe Bay: A case study in mixed-wet reservoirs", SPE 28576, presented at the SPE Annual Conference and Exhibition, New Orleans, LA, Sept. 1994.
19. Rueslåtten, H., Øren, P.E., Rosenberg, E., and Cuiec, L.: "A Combined Use of CRYO-SEM and NMR for Studying the Distribution of Oil and Brine in Sandstones," paper SPE/DOE 27804, presented at the SPE/DOE Symposium on IOR, Tulsa, OK, April 1994.

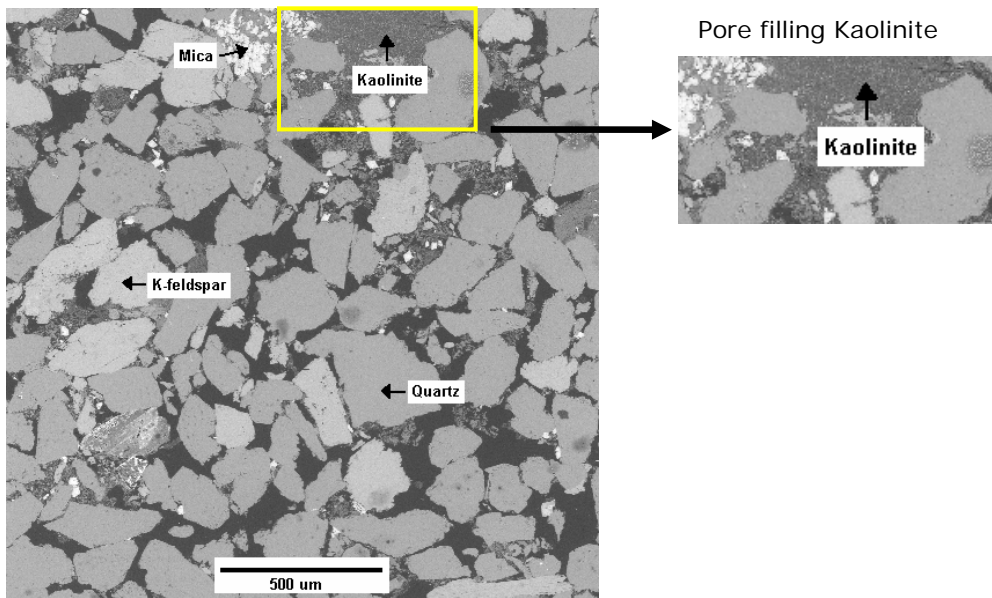


Figure 5: Thin section image for the MWL reservoir. Small pores consist of pore filling water-wet kaolinite.

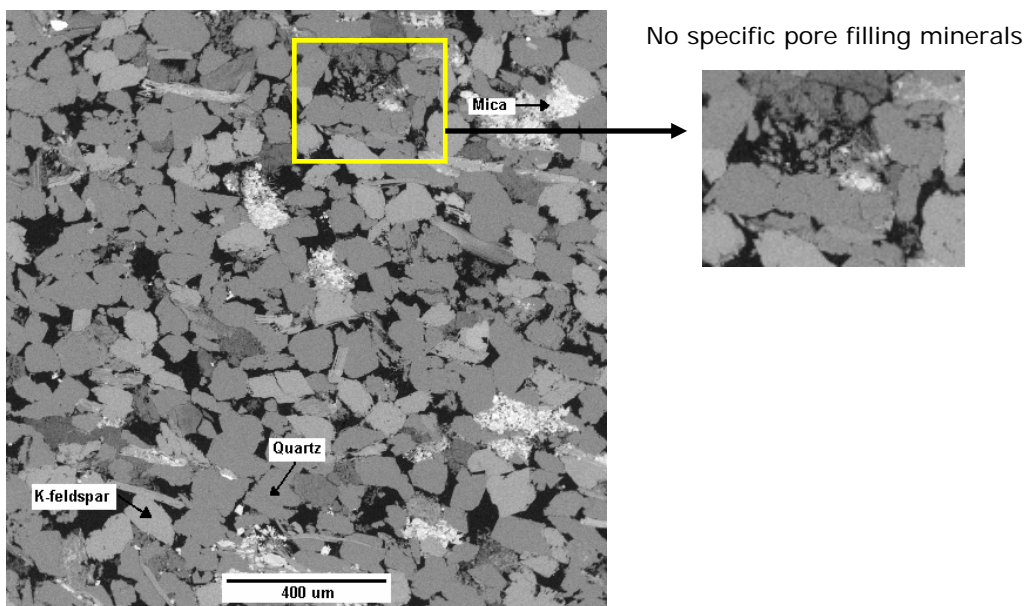


Figure 6: Thin section image for the MWS reservoir

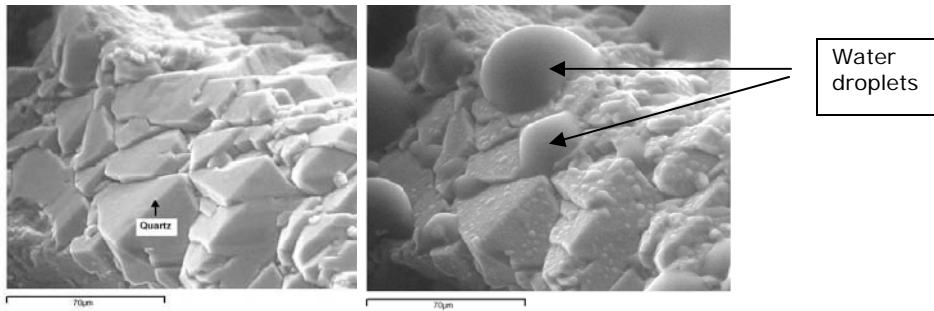


Figure 7; Quartz MWL , less water-wet as seen from the condensation (picture to the right) Water droplets (see arrows) formed during condensation.

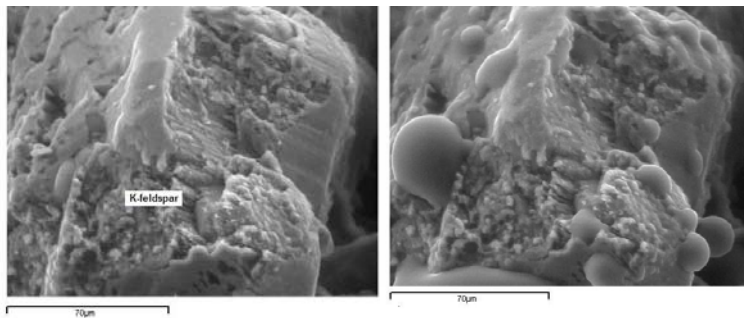


Figure 8: K-feldspar MWL, less water-wet as seen from the condensation (picture to the right) (as Fig. 7, water drops formed during condensation)

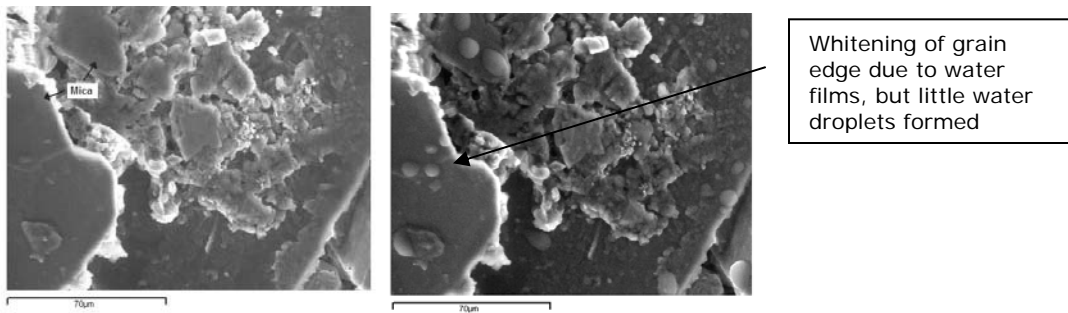


Figure 9: Mica MWL, water-wet as seen from the condensation (picture to the right)

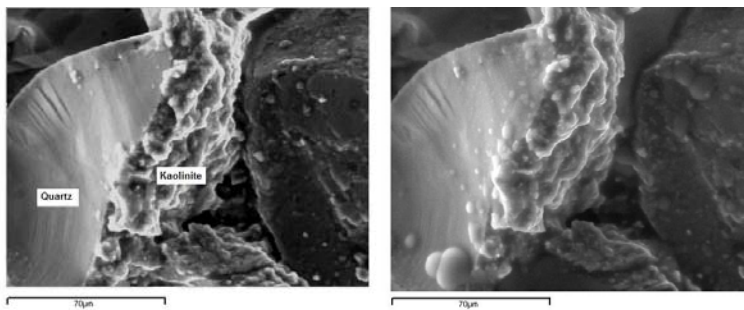


Figure 10: Kaolinite MWL, water-wet as seen from the condensation (picture to the right) (as Fig. 8, Whitening of grain edge due to water films, but little water droplets)

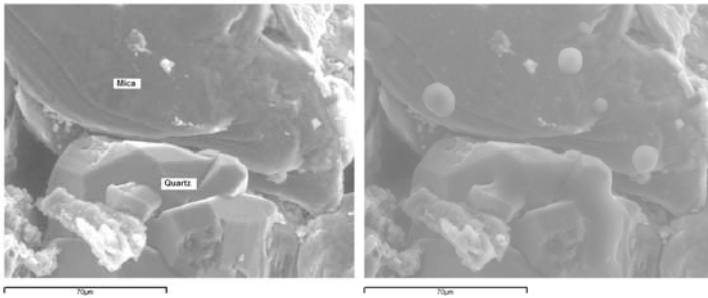


Figure 11: Quartz and mica MWS, water-wet quartz as seen from the condensation (picture to the right)

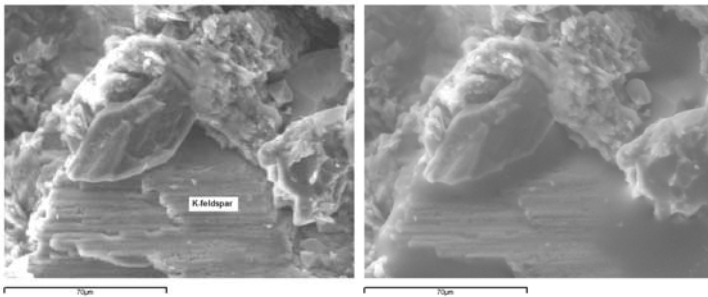


Figure 12: K-feldspar MWS, water-wet as seen from the condensation (picture to the right)

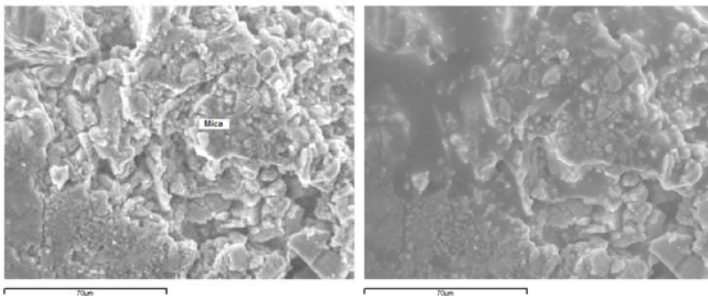


Figure 13: Mica MWS, less water-wet as seen from the condensation (picture to the right)

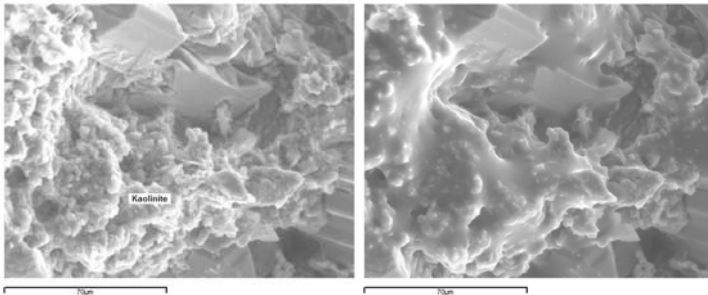


Figure 14: Kaolinite MWS, water-wet as seen from the condensation (picture to the right)